Parameter Sensitivity and Bistability in a Caspase Activation Model of Apoptosis

Megan Dowdell
REU in Algebraic Methods in Computational Biology
Texas A&M University, Summer 2025

Final Report: July 17, 2025

Abstract

How do cells decide between survival and self-destruction? This project explores that question using a mathematical model of apoptosis, the programmed cell death pathway. We use the 8-dimensional caspase network introduced by Eissing et al. and symbolically reduce it to a 2D model centered on Caspase-3 and Caspase-8 dynamics. This reduced system preserves key bistable features and enables efficient and accurate simulation, nullcline analysis, and steady-state classification. We also explore a further simplification to a 1D model, but find that it produces biologically implausible results, such as negative concentrations, and ultimately fails to capture the system's switching behavior. By performing parameter sweeps using our 2D model, we rank reactions based on their bistability windows, revealing which rates are most sensitive to disruption. We identify distinct dynamic behaviors resulting from individual parameter eliminations and find that only the inhibitory feedback associated with parameter ℓ_{11} can be removed without destroying bistability. These results demonstrate how mathematical models can uncover the key mechanisms that govern biological decision-making, and they lay the groundwork for future experimental validation.

1 Biological Background

1.1 Apoptosis and Caspase Signaling

Apoptosis, or programmed cell death, is the process by which organisms remove damaged or unnecessary cells. It's essential for development, immune function, and tissue health. If apoptosis is blocked, cells may survive when they shouldn't, which is a common feature in cancer.

Caspase proteins play a central role in apoptosis. Caspase-8 (C8) activates Caspase-3 (C3), which commits the cell to death. This cascade is known to behave like a switch: once activation starts, the process completes irreversibly.

These signaling events are not linear chains, they often involve feedback loops, inhibition, and scaffold proteins that affect how sharply and reliably the decision is made. This makes

apoptosis an ideal candidate for mathematical modeling, where we can test whether such features are sufficient to explain the irreversible "point of no return" observed experimentally.

We aim to understand this switch-like behavior using mathematical modeling. In particular, we study whether the caspase model shows **bistability**, where two different stable outcomes are possible under the same conditions.

1.2 Biochemical Reaction Networks

To analyze apoptosis using mathematics, we follow the framework introduced by Eissing et al. [1], who were among the first to model caspase signaling as a biochemical reaction network. In this approach, molecular interactions are represented as chemical reactions governed by rate laws, forming what is known as a **biochemical reaction network (BRN)**, a modeling strategy that uses species, reactions, and kinetics to simulate cellular behavior.

In a BRN, each reaction has a form:

$$A + B \underset{\ell_1}{\overset{k_1}{\rightleftharpoons}} C$$

which is governed by mass-action kinetics, producing rate laws:

$$r_1 = k_1[A][B]$$
$$r_2 = \ell_1[C]$$

This captures both the forward production of C from A and B, and its reverse conversion back, with rates governed by k_1 and ℓ_1, respectively. In modeling apoptosis, a BRN approach allows us to represent interactions such as Caspase-8 activating Caspase-3, IAPs inhibiting active caspases, and scaffold complexes that affect apoptotic activation. We translate each biological process into a reaction, and each reaction into an equation term, which creates a system that captures the emergent behavior of the whole network.

Each of these rate laws contributes a term in a differential equation, leading to a system of ODEs that describes the full time evolution of the species. One of the first such models of apoptosis using this approach was developed by Eissing et al. [1], who constructed a mass-action network capturing key caspase interactions and showed that it could exhibit bistable behavior. These ODEs will appear later in this paper and form the basis of our model. This modeling strategy allows us to analyze system-wide behavior including steady states, feedback loops, and switch-like decisions using mathematical tools and simulations. In this study, we extend the Eissing framework by applying symbolic reduction, nullcline analysis, and parameter sensitivity techniques to uncover new insights into the system's bistability.

2 Model Development

2.1 Caspase Activation Network

Our model, originally developed by Eissing et al. [1], consists of 8 molecular species and 13 reactions, encompassing activation, inhibition, binding, and feedback mechanisms. In this study, we work with the fully extended version of their model, which includes all 8 species

and all 13 reactions, rather than a simplified core network. The complete set of species is listed in Table 1, and a diagram of the full reaction network is shown in Figure 1, with species roles also detailed in the table.

Species (x_i)	Biological Role
x_1	Procaspase-8 (inactive)
x_2	Active Caspase-8
x_3	Procaspase-3 (inactive)
x_4	Active Caspase-3 (executioner)
x_5	Inhibitor of Apoptosis Protein (IAP)
x_6	Caspase-3–IAP complex
x_7	CARP scaffold complex
x_8	Caspase-8*–CARP complex

Table 1: Species and their roles in the model.

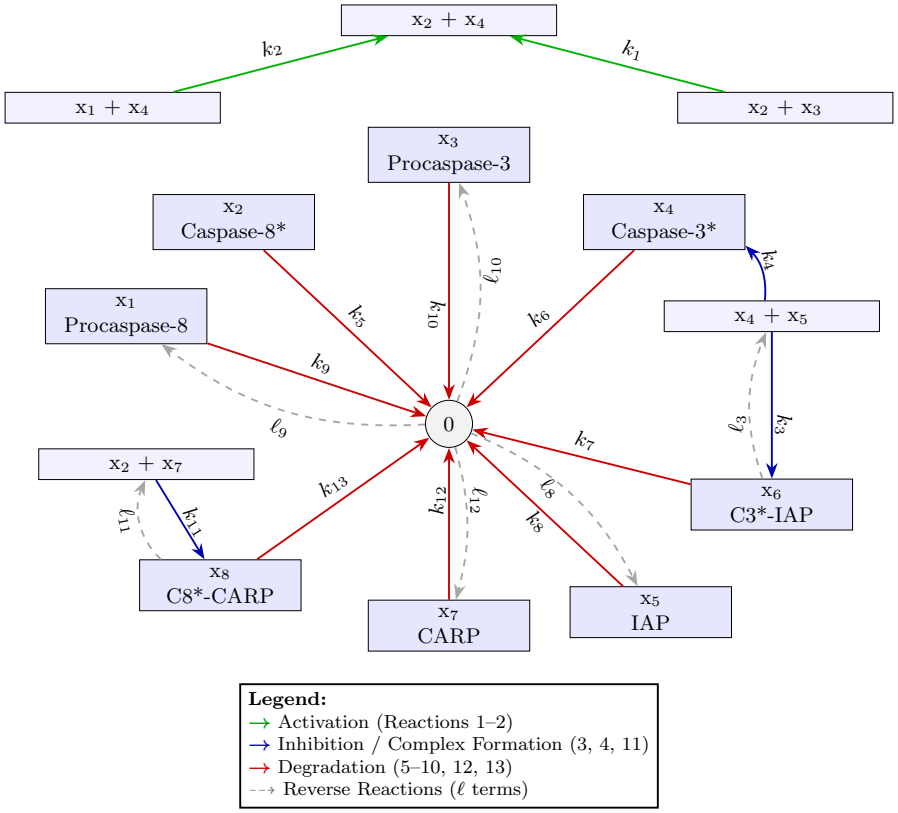

Figure 1: Reaction network for the extended caspase activation model.

Figure 1 illustrates several important structural features. At the top, reactions k_1 and k_2 form a **positive feedback loop** between active Caspase-8 (x_2) and active Caspase-3 (x_4), reinforcing their mutual activation. This feedback loop is central to bistable dynamics and underlies the system's potential for switch-like responses.

The **reverse reactions** in Figure 1 are each controlled by a rate parameter ℓ_i. These model reversible biological processes like dissociation or baseline production. Their inclusion ensures the system can settle into stable and biologically meaningful outcomes.

Inhibition is implemented through complex formation: active Caspase-3 binds IAP to form an inactive complex (x_6), and Caspase-8 binds the CARP scaffold to form x_8. These interactions reduce the availability of active caspases, dampening the apoptotic response.

2.2 Mass-Action ODE System

$$
\begin{aligned}
\frac{dx_1}{dt} &= -k_2 x_1 x_4 - k_9 x_1 + \ell_9, \\
\frac{dx_2}{dt} &= k_2 x_1 x_4 - k_5 x_2 - k_{11} x_2 x_7 + \ell_{11} x_8, \\
\frac{dx_3}{dt} &= -k_1 x_2 x_3 - k_{10} x_3 + \ell_{10}, \\
\frac{dx_4}{dt} &= k_1 x_2 x_3 - k_3 x_4 x_5 - k_6 x_4 + \ell_3 x_6, \\
\frac{dx_5}{dt} &= -k_3 x_4 x_5 - k_4 x_4 x_5 - k_8 x_5 + \ell_3 x_6 + \ell_8, \\
\frac{dx_6}{dt} &= k_3 x_4 x_5 - k_7 x_6 - \ell_3 x_6, \\
\frac{dx_7}{dt} &= -k_{11} x_2 x_7 - k_{12} x_7 + \ell_{11} x_8 + \ell_{12}, \\
\frac{dx_8}{dt} &= k_{11} x_2 x_7 - k_{13} x_8 - \ell_{11} x_8.
\end{aligned}
$$

[1]

These differential equations are derived directly from the mass-action reaction network shown in Figure 1. They describe the time evolution of each species in the system based on the kinetic rates of the reactions ($k_i$and ℓ_i).

This system defines the **extended caspase activation model** originally proposed by Eissing et al. [1]. The original model included a core subsystem of six species (x_1–x_6) representing the main apoptotic interactions between Caspase-8, Caspase-3, and IAPs. The extended version, used in our study, adds two more species (x_7 and x_8), along with Reactions 11–13. These additions introduce new regulatory mechanisms and feedback loops not present in the core model.

All simulations and analyses in this paper are based exclusively on the full 8-dimensional (8D) extended model. This system serves as the foundation for all symbolic reductions, steady-state classification, parameter sweeps, and elimination experiments described in the following sections.

3 Mathematical Analysis

3.1 Steady States in Dynamical Systems

A **steady state** of a dynamical system occurs when the concentration of every species remains constant over time. Mathematically, this means that all time derivatives vanish:

$$\frac{dx_i}{dt} = 0 \quad \text{for all } x_i.$$

In biological systems, steady states represent long-term outcomes such as survival or cell death.

Steady states can be classified based on their **stability**:

- **Stable:** If the system is slightly perturbed, it returns to the same steady state. These are like "valleys" in an energy landscape.
- **Unstable:** If perturbed, the system diverges away from the steady state. These correspond to "peaks" or saddle points.

This behavior is illustrated in Figure 2, where valleys represent stable configurations and peaks represent unstable ones.

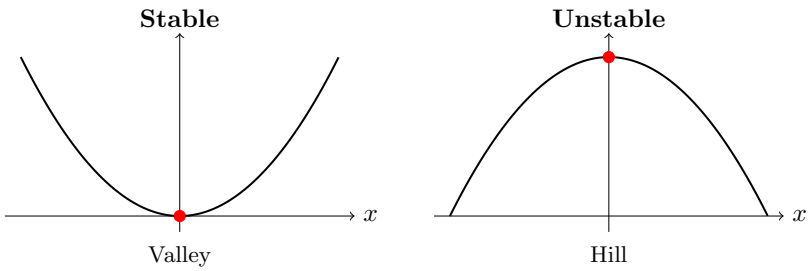

Figure 2: Energy landscape interpretation of stability. Valleys correspond to stable steady states; peaks represent unstable ones.

Understanding the number and stability of steady states is essential for detecting **bistability**: the presence of two stable outcomes under the same parameter conditions. In our model, this corresponds to a choice between survival and apoptosis.

3.2 Understanding Bistability and Feedback

A dynamical system is said to exhibit **bistability** if it has two or more **stable steady states** under the same set of parameter values. This means the system can settle into either of two long-term outcomes depending on its initial state or perturbations during its evolution. In biological contexts, bistability underlies many irreversible decision-making processes such as cell fate commitment, differentiation, and apoptosis.

Bistable systems typically contain an **unstable steady state** that separates the two basins of attraction. This unstable point acts as a decision threshold: small changes near it can push the system toward one stable state or the other. In many biological models, this intermediate state is a **saddle point**, which is a type of unstable equilibrium that is stable in one direction and unstable in another. While saddle points can attract trajectories along specific directions, they ultimately cannot hold the system long-term, and thus are not stable outcomes. As a result, bistable systems

can function like biological switches, remaining stable in one configuration until a signal pushes them over the threshold into a new state. This bistable switching behavior has been extensively discussed in biological decision models, including apoptosis and differentiation mechanisms [2].

In our apoptotic model, the two stable steady states correspond to the biological outcomes identified by Eissing et al. [1]:

- **Survival:** Low levels of active Caspase-3 (x_4), representing no cell death
- **Apoptosis:** High levels of active Caspase-3, indicating irreversible execution

This switch-like behavior is illustrated in Figure 3, which shows two stable valleys (survival and apoptosis) separated by a central unstable peak. The position of the unstable threshold depends on initial caspase levels and key reaction parameters.

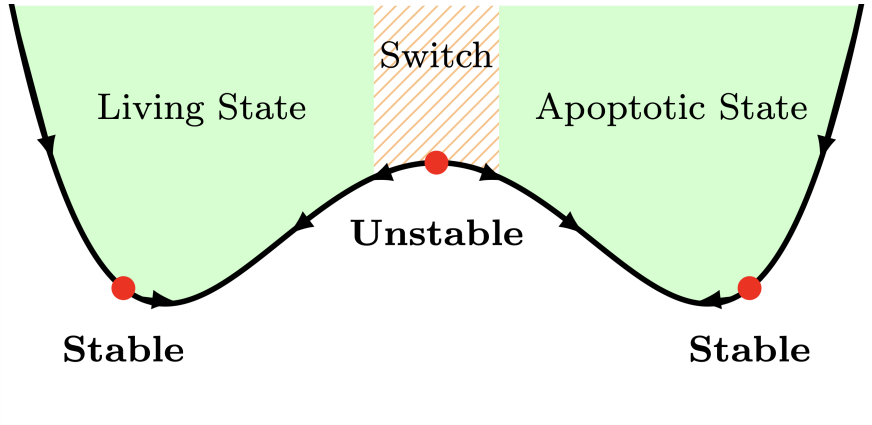

Figure 3: Conceptual diagram of bistability. Two stable steady states (living, apoptotic) are separated by an unstable threshold.

3.3 Waldherr et al. Sensitivity Analysis

To understand the system's steady-state behavior and its ability to commit to cell death, we analyze which species have the greatest influence on the network. Waldherr et al. (2007) performed a parameter sensitivity analysis by computing normalized sensitivity coefficients, which measure how much steady-state concentrations of each species respond to small changes in individual parameters. Species were ranked by the overall magnitude of these sensitivities to identify which species and reactions most strongly influence the system's behavior.

The results are shown in the chart below, which visualizes each species' relative importance in driving the network dynamics.

The analysis identified four species as most influential:

- x_2 — Active Caspase-8
- x_4 — Active Caspase-3
- x_6 — Caspase–3–IAP complex
- x_8 — Caspase–8*–CARP complex

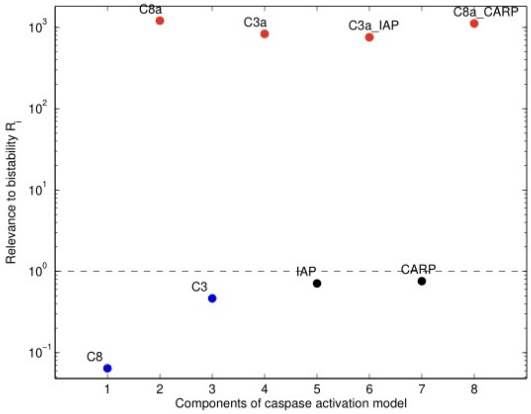

Figure 4: Species sensitivity from [3], Figure 3 of their original publication.

Waldherr constructed the following reduced model using only the ODEs for the above species.

Reduced ODEs (4-variable system):

$$\dot{x}_2 = \frac{k_9 k_2 x_4}{k_9 + k_2 x_4} - k_5 x_2 - \frac{(k_{12} + k_{11} x_8) k_{11} x_2}{k_{12} + k_{11} x_2} + \ell_{11} x_8$$

$$\dot{x}_4 = \frac{k_{10} k_1 x_2}{k_{10} + k_1 x_2} - \frac{(k_8 + k_3 x_6) k_3 x_4}{(k_3 + k_4) x_4 + k_8} + k_3 x_6 - k_6 x_4$$

$$\dot{x}_6 = \frac{(k_8 + k_3 x_6) k_3 x_4}{(k_3 + k_4) x_4 + k_8} - k_3 x_6 - k_7 x_6$$

$$\dot{x}_8 = \frac{(k_{12} + k_{11} x_8) k_{11} x_2}{k_{12} + k_{11} x_2} - k_{11} x_8 - k_{13} x_8$$

3.4 Two-Species Symbolic Reduction

To identify steady states of the system, we begin by setting all time derivatives $\dot{x}_i = 0$, transforming the full 8-dimensional ODE system into a set of algebraic equations. Solving this system symbolically is challenging due to its complexity. Following the strategy proposed by Waldherr et al. [3], we analytically eliminate six of the eight species by expressing their steady-state concentrations in terms of just two variables: active Caspase-8 (x_2) and active Caspase-3 (x_4). These two variables are chosen for their biological and mathematical importance, as they form the core positive feedback loop (Reactions k_1 and k_2) that drives apoptotic switching behavior.

To perform the reduction, we first solve the steady-state equations for the remaining species $x_1, x_3, x_5, x_6, x_7, x_8$, obtaining their symbolic expressions in terms of x_2 and x_4. We then substitute these into the original differential equations for $\dot{x}_2$ and $\dot{x}_4$, yielding a two-dimensional system. The full symbolic expressions and source code used to generate this reduction are available in the GitHub repository cited in [4].

The resulting reduced equations are:

$$\dot{x}_2 = \frac{-k_{11}k_{13}\ell_{12}x_2(k_2x_4+k_9) + k_2\ell_9x_4(k_{11}k_{13}x_2+k_{12}k_{13}+k_{12}\ell_{11}) - k_5x_2(k_2x_4+k_9)(k_{11}k_{13}x_2+k_{12}k_{13}+k_{12}\ell_{11})}{(k_2x_4+k_9)(k_{11}k_{13}x_2+k_{12}k_{13}+k_{12}\ell_{11})}$$

$$\dot{x}_4 = \frac{(k_1\ell_{10}x_2 - k_6x_4 - k_3k_7\ell_8x_4)(k_3k_7x_4+k_4k_7x_4+k_4\ell_3x_4+k_7k_8+k_8\ell_3)}{(k_1x_2+k_{10})(k_3k_7x_4+k_4k_7x_4+k_4\ell_3x_4+k_7k_8+k_8\ell_3)}$$

These expressions define a symbolic two-dimensional dynamical system that forms the foundation for our nullcline plots, steady-state analysis, and bistability classification in subsequent sections. Retaining the feedback loop between Caspase-8 and Caspase-3 allows the reduced model to capture the essential nonlinear dynamics of the full 8D system while enabling symbolic simplification and computational analysis.

4 Simulations and Results

To explore the behavior of the caspase activation model, we implemented simulations in Python. Symbolic manipulations and reductions were performed using `SymPy` [5], while numerical evaluations and plots were generated using `NumPy` [6] and `Matplotlib` [7]. This framework enabled us to simulate nullclines, compute steady states, run parameter sweeps, and classify stability efficiently and reproducibly. The following subsections walk through our key computational results, beginning with how different parameter choices control monostability versus bistability. The full codebase is available on GitHub [4].

4.1 Parameter Setup for Bistability

We use the parameter values from [3] as a baseline configuration for the reduced system. These values were chosen by the authors of [3] to reflect biologically reasonable dynamics, but under this setup, the system exhibits only **monostable** behavior as shown in Figure 5.

Table 2: Parameter values (Col 2: Waldherr et al. [3], Col 3: Modified values).

Parameter	**Waldherr et al. (2007)**	**Modified Set**
k_1	$5.8 \cdot 10^{-5}$	*$1.42 \cdot 10^{-5}$*
k_2	$1.0 \cdot 10^{-5}$	$1.0 \cdot 10^{-5}$
k_3	$5.0 \cdot 10^{-4}$	$5.0 \cdot 10^{-4}$
k_4	$3.0 \cdot 10^{-4}$	$3.0 \cdot 10^{-4}$
k_5	$5.8 \cdot 10^{-3}$	$5.8 \cdot 10^{-3}$
k_6	$5.8 \cdot 10^{-3}$	$5.8 \cdot 10^{-3}$
k_7	$1.73 \cdot 10^{-2}$	$1.73 \cdot 10^{-2}$
k_8	$1.16 \cdot 10^{-2}$	$1.16 \cdot 10^{-2}$
k_9	$3.9 \cdot 10^{-3}$	$3.9 \cdot 10^{-3}$
k_{10}	$3.9 \cdot 10^{-3}$	$3.9 \cdot 10^{-3}$
k_{11}	$5.0 \cdot 10^{-4}$	$5.0 \cdot 10^{-4}$
k_{12}	$1.0 \cdot 10^{-3}$	$1.0 \cdot 10^{-3}$
k_{13}	$1.16 \cdot 10^{-2}$	$1.16 \cdot 10^{-2}$
ℓ_3	0.21	0.21
ℓ_8	464	464
ℓ_9	507	507
ℓ_{10}	81.9	81.9
ℓ_{11}	0.21	0.21
ℓ_{12}	540	*440*

To induce bistability, we made two minimal but impactful modifications: we *increased* k_1, the rate at which Caspase-8 activates Caspase-3, thereby strengthening the positive feedback loop. Simultaneously, we *decreased* ℓ_{12}, which governs the reactivation of CARP, a downstream apoptotic

inhibitor. See Table 2. Together, these changes increase the strength of activation and reduce inhibition, making bistable behavior possible in the caspase activation model.

4.2 Nullclines: Monostable vs Bistable Cases

We analyze the steady-state structure of the reduced 2D system by plotting its **nullclines**, which are curves where $\dot{x}_2 = 0$ or $\dot{x}_4 = 0$.

- The $\dot{x}_2 = 0$ nullcline represents values where Caspase-8 ($\dot{x}_2$) concentration is steady.
- The $\dot{x}_4 = 0$ nullcline represents values where Caspase-3 ($\dot{x}_4$) concentration is steady.
- Intersections indicate steady states; stability is later classified via Jacobian analysis.

Using the full parameter set listed in Table 2, we simulate the system's behavior under these fixed kinetic conditions. By plotting the nullclines of the reduced two-dimensional system, we identify where the time derivatives $\dot{x}_2$ and $\dot{x}_4$ simultaneously vanish. These intersection points represent steady states, which are potential long-term outcomes of the system that will later be classified as stable or unstable. Under the original Waldherr et al. parameters, only one intersection appears, indicating **monostability**. See Figure 5.

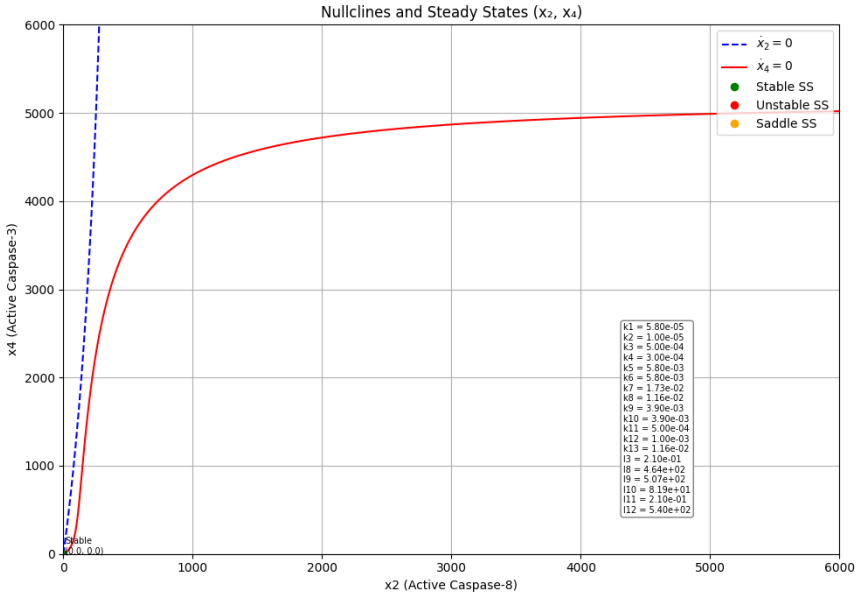

Figure 5: Nullcline plot under original parameters showing a single (monostable) steady state.

With the **modified parameters**, the nullclines intersect at three distinct points: two are stable, and one is unstable. This confirms **bistability** in the reduced system (Figure 6). To determine the stability of each equilibrium state, our simulation framework includes automatic classification based on Jacobian eigenvalue analysis, described in the following section.

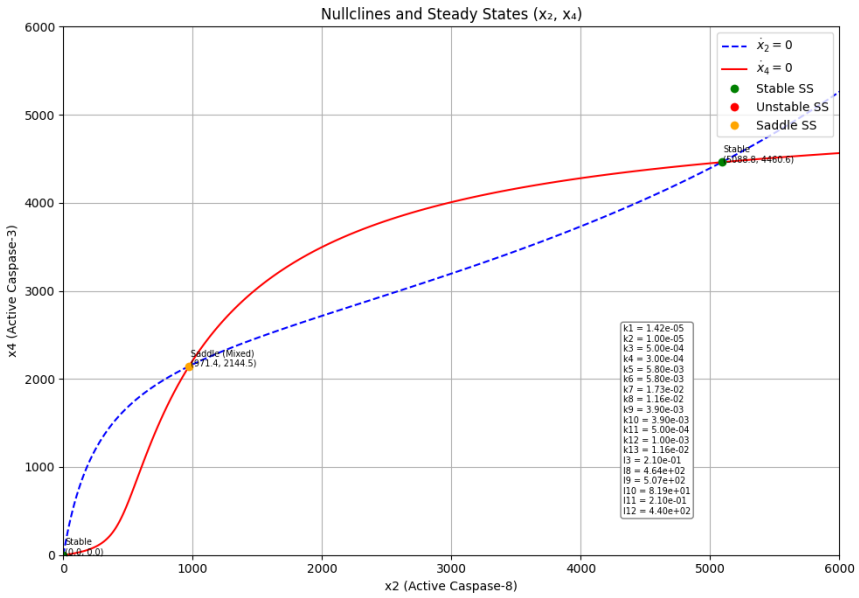

Figure 6: Nullcline plot with modified parameters showing two stable steady states separated by an unstable one.

4.3 Steady State Verification (2D vs 8D)

Each steady state corresponds to an intersection point of the nullclines $\dot{x}_2 = 0$ and $\dot{x}_4 = 0$ in the reduced model. To classify the stability of each equilibrium, we analyze the local dynamics using the Jacobian matrix:

$$J(x_2, x_4) = \begin{bmatrix} \frac{\partial \dot{x}_2}{\partial x_2} & \frac{\partial \dot{x}_2}{\partial x_4} \\ \frac{\partial \dot{x}_4}{\partial x_2} & \frac{\partial \dot{x}_4}{\partial x_4} \end{bmatrix}$$

We compute the eigenvalues λ_1, λ_2 of J at each nullcline intersection and classify the steady states based on the sign of the real parts:

$\mathbf{Re}(\lambda_1), \mathbf{Re}(\lambda_2) < 0$**:**	Stable (attracts nearby trajectories)
$\mathbf{Re}(\lambda_1) < 0 < \mathbf{Re}(\lambda_2)$**:**	Saddle (partially stable; repels in one direction)
$\mathbf{Re}(\lambda_1), \mathbf{Re}(\lambda_2) > 0$**:**	Unstable (repels in all directions)

Classification based on Jacobian eigenvalues [8].

To ensure the reduced system accurately represents the full model, we also compute the Jacobian matrix and corresponding eigenvalues of the original 8-dimensional system at the same steady-state locations, the values of x_2 and x_4 obtained from the 2D nullcline intersections. The values of the remaining six species $(x_1, x_3, x_5, x_6, x_7, x_8)$ are recovered by back-substituting those x_2 and x_4 values into the symbolic expressions derived during the reduction process. This allows us to reconstruct the full 8D steady-state vector and evaluate whether the reduced system preserves the qualitative dynamics of the complete model.

Steady State	2D Eigenvalues	8D Real Parts	Classification
Low (0, 0)	$\lambda_1 = -11.56,\ \lambda_2 = -1.49$	All negative	**Stable**
Middle (971.4, 2144.5)	$\lambda_1 = -0.037,\ \lambda_2 = +0.008$	Mixed (1 positive)	**Saddle**
High (5088.8, 4460.6)	$\lambda_1 = -0.0087,\ \lambda_2 = -0.0036$	All negative	**Stable**

Table 3: Eigenvalue-based classification of steady states from both reduced and full systems, corresponding to the parameters and nullcline intersections shown in Figure 6.

These results confirm bistability under the modified parameter set and demonstrate that the reduced symbolic model reliably mirrors the behavior of the full 8D system. If the classifications had not matched, it would have indicated that the reduction failed to preserve key features of the system and is not biologically accurate.

4.4 One-Species Reduction and Failure Analysis

To further simplify the model, we attempted a one-species reduction by eliminating all variables except x_4 (active Caspase-3). The goal was to derive a single symbolic equation $\dot{x}_4 = f(x_4)$ by substituting all other variables at steady state.

To attempt a one-species reduction, we began with the two-dimensional reduced system involving $\dot{x}_2$ and $\dot{x}_4$. By setting both derivatives equal to zero, we obtained a pair of algebraic steady-state equations that describe the system's behavior at equilibrium. We solved the steady-state equation $\dot{x}_2 = 0$ to express x_2 as a function of x_4, and substituted that expression into $\dot{x}_4$. This yielded a single symbolic equation $\dot{x}_4 = f(x_4)$ in terms of Caspase-3 alone.

The resulting equation was highly nonlinear, containing rational functions, nested radicals, and large symbolic terms in x_4, k_i, and ℓ_i:

$$\dot{x}_4 = \frac{\text{large polynomial in } x_4 \text{ and } k_i, \ell_i, \text{ including } \sqrt{\cdots}}{\text{rational denominator in } x_4} + \cdots$$

To identify steady states, we solved $\dot{x}_4 = 0$ numerically and plotted the resulting nullcline (Figure 7). Due to the complexity of the function, this equation sometimes yielded one or two roots, indicated as branches in the 1D phase plane plots.

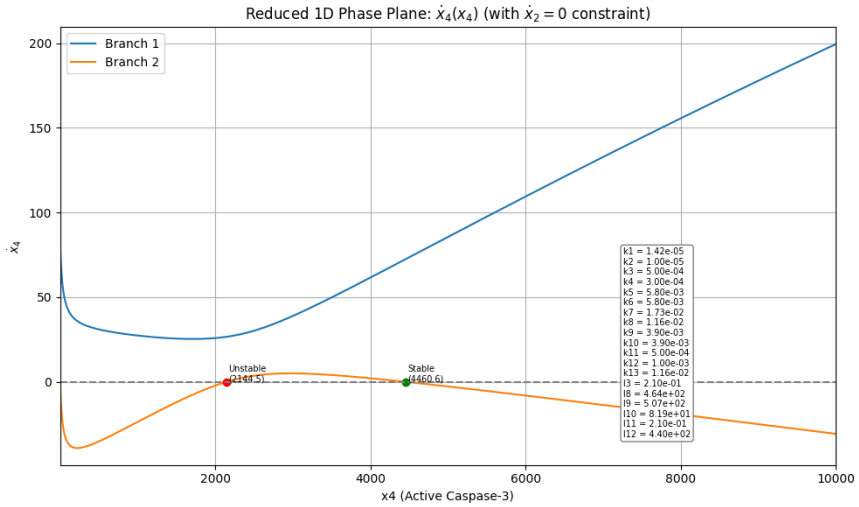

Figure 7: One-species reduction fails to reproduce bistability. Only a single steady state is detected.

Stability of each root was inferred from the slope of $\dot{x}_4(x_4)$ at the crossing point:

- Negative slope $\Rightarrow$ stable steady state
- Positive slope $\Rightarrow$ unstable steady state

However, to assess biological plausibility, we back-substituted these x_4 values into the full model to solve for the corresponding x_2. In several cases, this yielded negative concentrations:

$$x_2 = -2908.97 \qquad (x_4 = 2144.48)$$
$$x_2 = -603.54 \qquad (x_4 = 4460.63)$$

These values are biologically implausible. The one-species model fails to preserve the coupling between Caspase-8 (x_2) and Caspase-3 (x_4), making it unsuitable for studying bistability or apoptotic commitment.

Conclusion: The one-species model cannot replicate bistability or yield biologically meaningful steady states. At least two species must be retained for accurate and interpretable analysis.

4.5 Parameter Sweeps and Bifurcation Insights

To better understand the conditions that enable bistability in our model, we performed systematic parameter sweeps. This approach involves varying one parameter at a time and examining how the system's steady states and their stability change as a result. The aim is to identify bifurcation points: critical parameter values at which the number or nature of steady states shifts dramatically.

Bifurcations represent qualitative transitions in system behavior. For instance, a system may move from monostability to bistability, or lose all steady states entirely. These transitions are essential in biological systems that require sharp, switch-like decisions, such as the irreversible commitment to apoptosis.

Parameter sweeps also help identify which reaction rates are most influential in maintaining bistability. Following the approach of Albeck et al. [9], we analyzed how varying key parameters shapes the underlying dynamics, especially feedback-driven behaviors involved in caspase regulation.

Goal: Determine which reaction rates control the cell's ability to make all-or-nothing life-or-death decisions.

Bifurcation Diagram for k_1

We first varied the parameter k_1, which governs how efficiently active Caspase-8 activates Caspase-3, while keeping all other parameters set to the modified parameter set in Table 2. This parameter plays a crucial role in controlling the positive feedback loop responsible for switching the system into an apoptotic state [1].

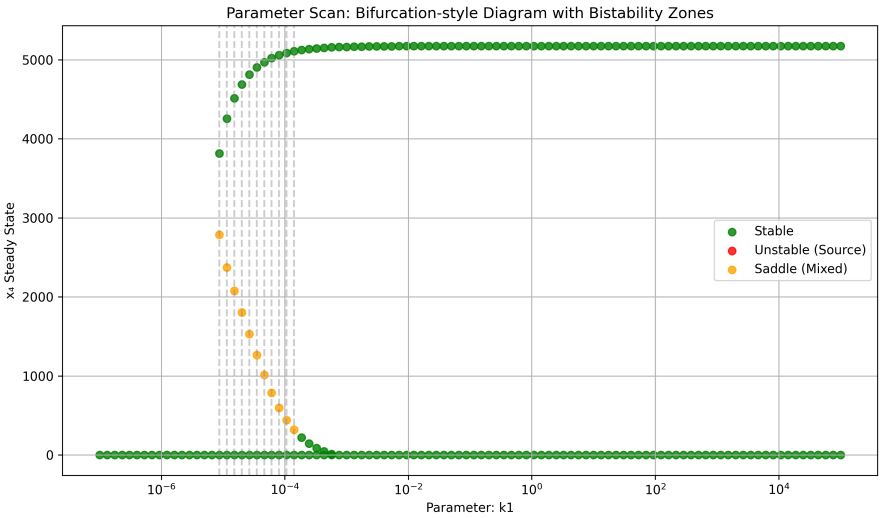

Figure 8: Bifurcation diagram showing steady-state x_4 values as a function of k_1.

As shown in Figure 8, the system exhibits a bifurcation: for low k_1, only a low steady-state Caspase-3 level is possible (representing survival); as k_1 increases beyond a threshold, a high Caspase-3 level emerges, signifying apoptosis. In the intermediate region, bistability is observed, where both fates are possible depending on initial conditions.

Saddle points are a type of unstable steady state that act as thresholds between basins of attraction. During a bifurcation, a saddle can merge with a previously stable steady state, causing that point to become unstable. However, this change may not be visible in a bifurcation diagram. For instance, in our bifurcation sweep of k_1, the lower branch appears to remain stable across the entire parameter range. But when we analyzed nullclines at representative k_1 values, we found that in the high-k_1 regime, the lower steady state had actually become a saddle. The bifurcation plot continued to display it in green due to trajectory behavior near $(0, 0)$, where simulations remained trapped.

To distinguish true attractors from unstable saddles, we use nullcline intersections and local eigenvalue classification. Full sweep results and nullcline plots for each parameter are provided in Appendix A.

Nullcline Plots at Representative k_1 Values

To visualize the bifurcation more concretely, we plotted the nullclines of the reduced model at three representative k_1 values:

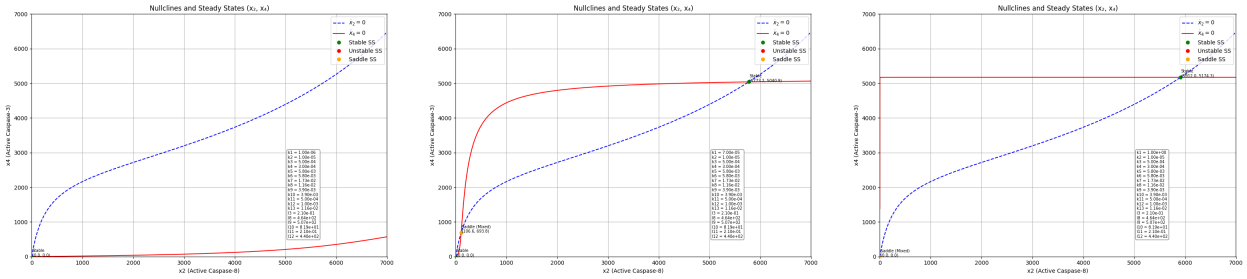

Zone 1: Low k_1 (Living Only) Zone 2: Middle k_1 (Bistable) Zone 3: High k_1 (Apoptosis Only)

Figure 9: Nullcline plots showing steady-state changes across low, middle, and high k_1 regimes.

While bifurcation diagrams show how steady-state values evolve as a parameter changes, nullcline plots reveal the underlying mechanism of how the system's stability shifts at each point along that curve. By examining individual nullcline snapshots across the parameter sweep, shown in Figure 8, we gain direct insight into the cell's decision landscape. At low k_1, the nullclines intersect at a single stable point, corresponding to a living cell fate. At intermediate k_1, three intersections emerge: two stable (living and apoptotic) separated by an unstable saddle point, which clearly indicates bistability. At high k_1, only the high-x_4 apoptotic attractor remains. These transitions validate the bifurcation structure and illustrate how system dynamics change qualitatively across regimes.

4.6 Key Parameters for the Apoptotic Switch

Bifurcation diagrams revealed how specific parameters, such as k_1, govern whether the system exhibits monostability or bistability. In each diagram, a range of values exists where the system transitions from a single stable steady state to three steady states (two stable, one unstable) and back again. We define this range as the **bistability window**. It represents the interval over which the system supports switch-like behavior where initial conditions determine whether the cell lives or undergoes apoptosis.

To quantify how sensitive each reaction is to this switch-like behavior, we computed the bistable window for all parameters individually. A smaller window indicates high sensitivity: even minor perturbations to the parameter value can destroy bistability. Conversely, a wider window suggests robustness.

This analysis reveals that certain parameters, such as (ℓ_9), (k_3), and (ℓ_{12}), exhibit very narrow bistable ranges, meaning even slight changes can disrupt bistability. These act as fragile "switches" in the apoptotic decision-making process. Contrarily, parameters like (k_{11}), (k_{13}), and (ℓ_{11}) exhibit broad bistable windows, suggesting the system is relatively insensitive to fluctuations in these values. The bistable window widths, quantified in terms of logarithmic span and percentage of the scanned range, are summarized in Table 4. Parameters are ordered from most to least sensitive.

Parameter	Lower Bound	Upper Bound	Log-Width	% of Scan
l9	4.98×10^{2}	8.70×10^{2}	0.24	2.0%
k3	8.11×10^{-5}	4.33×10^{-4}	0.73	6.1%
l12	7.05×10^{1}	3.76×10^{2}	0.73	6.1%
l10	9.33×10^{1}	4.98×10^{2}	0.73	6.1%
k4	3.27×10^{-4}	2.31×10^{-3}	0.85	7.1%
l3	2.01×10^{-1}	1.42	0.85	7.1%
k7	2.31×10^{-3}	1.63×10^{-2}	0.85	7.1%
l8	7.05×10^{1}	4.98×10^{2}	0.85	7.1%
k1	8.70×10^{-6}	1.42×10^{-4}	1.21	10.1%
k9	2.48×10^{-4}	4.04×10^{-3}	1.22	10.2%
k10	3.27×10^{-4}	5.34×10^{-3}	1.22	10.2%
k2	8.70×10^{-6}	1.87×10^{-4}	1.33	11.1%
k6	3.27×10^{-4}	7.05×10^{-3}	1.34	11.2%
k5	3.27×10^{-4}	1.23×10^{-2}	1.58	13.2%
k12	1.00×10^{-7}	2.85×10^{-2}	5.45	45.4%
k8	1.00×10^{-7}	4.64×10^{-1}	6.67	55.6%
l11	1.00×10^{-7}	5.72	7.76	64.7%
k13	4.33×10^{-4}	1.00×10^{5}	8.36	69.7%
k11	2.01×10^{-5}	1.00×10^{5}	9.70	80.8%

Table 4: Parameters with narrow bistable regions (e.g., **k3**, **l9**) act as key switches. Wide ranges (e.g., **k11**) indicate robust tolerance.

4.7 Nullcline Parameter Zeroing Method

To deepen our analysis of the nullcline zeroing approach, we categorized the system's stability responses after knocking out each parameter individually. Table 5 summarizes the resulting nullcline configurations and their biological implications.

Each parameter was set to zero and the nullclines $\dot{x}_2 = 0$ and $\dot{x}_4 = 0$ were recomputed. The outcome types reflect the number and type of steady states preserved, and whether the switch-like bistability was disrupted. The results indicate that most parameters are essential for maintaining bistability. Knocking them out results in a loss of apoptosis, a collapse of survival, or even the complete removal of any stable state. Only one parameter, ℓ_{11}, was found to be dispensable in that bistable dynamics are preserved.

To further illustrate the dynamic effects of parameter elimination, Appendix A contains individual nullcline plots for each zeroed system. These visualizations show how the qualitative structure of the phase portrait changes when bistability is lost. For instance, when $k_1 = 0$, the high apoptotic state disappears and only a survival steady state remains; when $k_9 = 0$, the opposite occurs, with only apoptosis remaining as an attractor. In cases such as k_{11} or ℓ_{13}, the resulting nullclines do not intersect in any biologically meaningful configuration, leaving the system without any stable state. These outcomes visually confirm and enrich the classifications in Table 5, providing intuition for how individual reactions shape the decision-making landscape of the apoptotic switch.

Table 5: **Effect of Parameter Elimination on Nullcline Structure and Bistability**

Outcome Type	Parameters Zeroed	Resulting Nullcline Behavior
Low stable only	k_1, k_2, k_4, ℓ_3, ℓ_9, ℓ_{10}	Cell is trapped in survival; apoptosis cannot occur
Low stable then saddle	k_5, k_6	Cell is locked in survival; saddle is non-functional
Low saddle then high stable	k_3, k_7, ℓ_8	Survival basin lost; unstable low region leads to apoptosis
Mid saddle then high stable	k_8, k_{12}	No survival state; flow from unstable middle leads to apoptosis
High stable only	k_9, k_{10}	Cell starts and ends in apoptosis; no other dynamics exist
Low saddle only	k_{11}, k_{13}, ℓ_{13}	No stable state; biologically implausible
Bistable	ℓ_{11}	Switch retained; bistability preserved

Color Legend:
Green = Activation (Reactions 1–2)
Blue = Inhibition / Complex Formation (Reactions 3, 4, 11)
Red = Degradation (Reactions 5–10, 12, 13)
Gray = Reverse Reactions (ℓ terms)

These results highlight the fragility of bistability in the apoptosis model and show how reaction type plays a critical role. In Table 5, parameters are grouped and color-coded by their biological function: activation, inhibition, degradation, or reversibility. The system is highly sensitive to the removal of most parameters, with each group showing different modes of bistability disruption. Activation parameters like k_1 and k_2 are essential for triggering apoptotic switching; removing them collapses the system to survival-only states. Degradation terms such as k_9 and k_{10} cause the opposite effect, locking the system in apoptosis. Inhibitory and complex-forming reactions lead to unstable or biologically implausible behavior when removed. Only one reverse reaction, ℓ_{11}, is dispensable without loss of bistability, revealing a minimal set of reactions required to preserve switch-like dynamics.

5 Conclusions and Future Work

5.1 Summary of Findings

This project analyzed bistability in a model of apoptotic signaling, focusing on how it emerges from the system's reactions and parameter structure. Eissing et al. [1] previously showed that feedback between caspases can create switch-like behavior in this network. Building on that foundation, we used symbolic reductions, steady-state analysis, and parameter perturbations to identify which reactions and rates are most important for generating and maintaining bistable outcomes.

Our parameter sweeps revealed that a small number of kinetic rates critically shape the range over which bistability is maintained. Reactions involving ℓ_9 and k_3 exhibited narrow bistable windows, where even modest changes destroyed switch-like behavior. In contrast, other rates such as k_{11} and k_{13} allowed for broader flexibility while preserving bistability. These findings build upon Eissing's original insights by quantifying how robustness varies across the reaction network.

We further analyzed bistability by individually removing parameters from the model and plotting nullclines of the reduced two-species system. In several cases, the system lost one or both stable steady states: some deletions caused the system to converge solely to survival, while others forced apoptosis. This analysis showed that while the full network supports robust switching, that behavior depends on specific combinations of feedback and interaction terms and removing certain parameters can completely abolish bistability.

We also tested symbolic model reductions to assess whether lower-dimensional representations could replicate the full model's dynamics. A two-species reduction, retaining Caspase-8 and Caspase-3, successfully preserved the system's steady-state structure and stability under our modified set of parameter values. However, a one-species reduction failed to do so. In many cases, it yielded negative concentrations for excluded variables, violating physical constraints and demonstrating that the reduction eliminated critical interactions.

Altogether, our findings suggest that the apoptotic switch relies on a finely balanced network, where multiple parameters and feedback interactions operate to show a clear separation between survival and death outcomes. In many cases, a wide range of parameter values still permitted bistable behavior, indicating a degree of tolerance within the system. At the same time, eliminating or modifying specific reactions, such as key activation or degradation steps, was enough to abolish bistability altogether.

5.2 Future Directions

Although this study is purely computational, future work could test whether the model's predictions hold in biological systems. In particular, time-course measurements of caspase activity and cell fate outcomes, under controlled perturbations, could help evaluate whether critical thresholds and bistable switching behaviors predicted by the model occur in real apoptotic pathways. Eissing et al. [1] combined mathematical modeling with experimental validation in cell lines, supporting the biological relevance of bistable dynamics in apoptosis. Similar experiments could be used to test the 2D version of our model.

Beyond single-parameter analysis, future studies could investigate how combinations of parameters influence bistability. Two-dimensional sweeps across pairs of reaction rates may reveal interactions that are not apparent in isolation. These interaction maps could provide deeper insight into how robustness and fragility emerge from interdependent reactions in the network.

Another direction is model refinement. One approach is to simplify the network further—such as removing the non-essential parameter ℓ_{11} or applying symbolic techniques to eliminate additional variables, while preserving bistable behavior. Alternatively, the model could be expanded to incorporate additional pathways, such as more caspases and signals that influence apoptotic regulation. These refinements may provide a more complete view of the signaling cascade and its behavior.

The methods used in this study could also be applied to other biological systems that involve binary decisions. Examples include immune activation, stem cell differentiation, and developmental processes where cells commit to one of two possible fates. Bistable dynamics are a common feature in these systems, often driven by feedback loops [10]. Extending this modeling approach to other contexts may help reveal whether similar switching mechanisms are at work and how they might vary across biological pathways or cell types.

Altogether, this work provides a foundation for analyzing the decision-making architecture of complex biological networks. By combining symbolic modeling, stability analysis, and parameter sensitivity, we offer tools for uncovering the principles that govern how cells make irreversible choices, insights that will be increasingly important as biological modeling moves closer to experimental and clinical applications.

A Appendix A: Parameter-Specific Plots

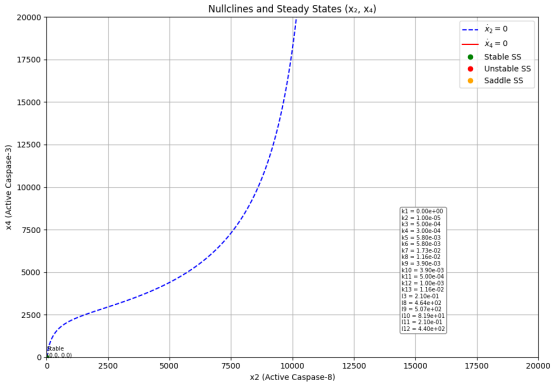

Nullcline: $k_1 = 0$

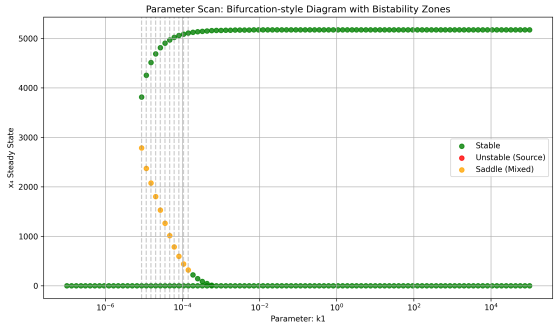

Sweep: k_1

Figure 10: Parameter k_1: elimination vs sweep

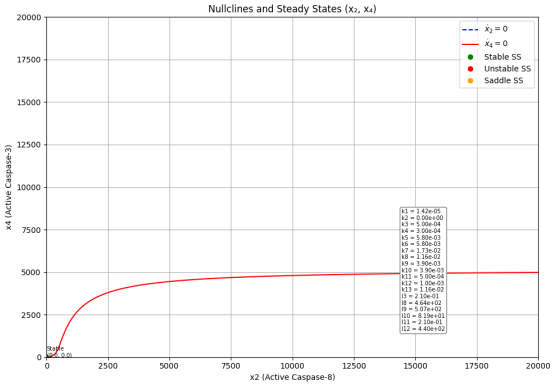

Nullcline: $k_2 = 0$

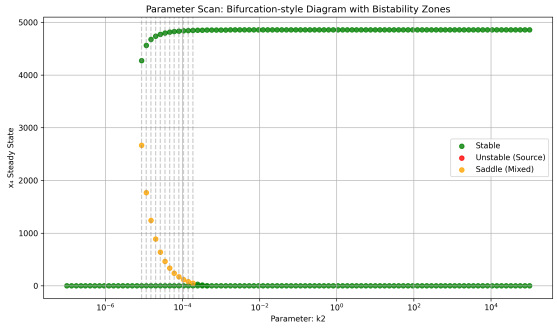

Sweep: k_2

Figure 11: Parameter k_2: elimination vs sweep

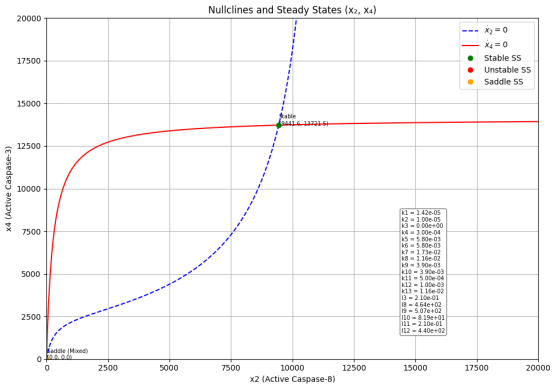

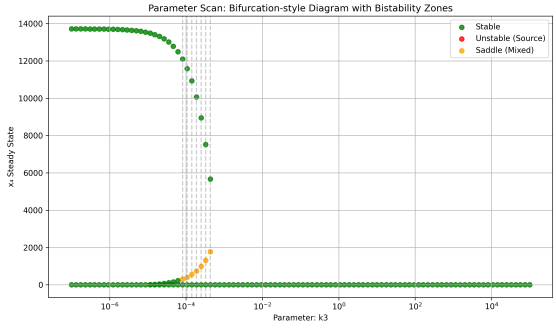

Nullcline: $k_3 = 0$ Sweep: k_3

Figure 12: Parameter k_3: elimination vs sweep

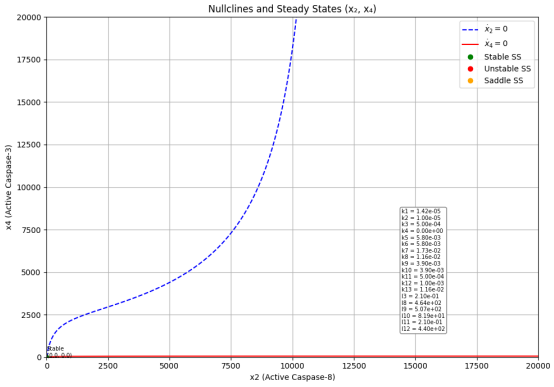

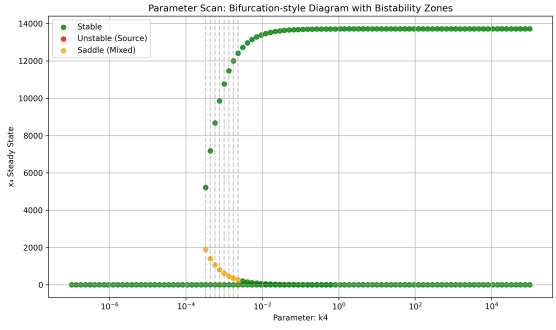

Nullcline: $k_4 = 0$ Sweep: k_4

Figure 13: Parameter k_4: elimination vs sweep

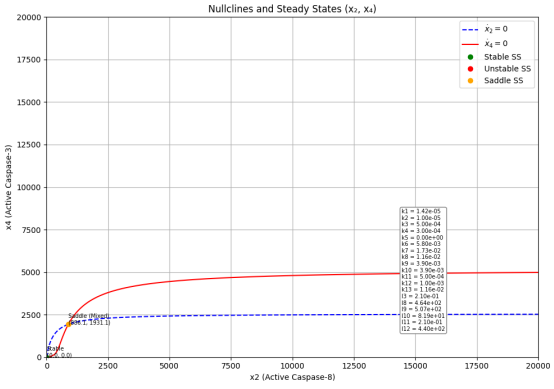

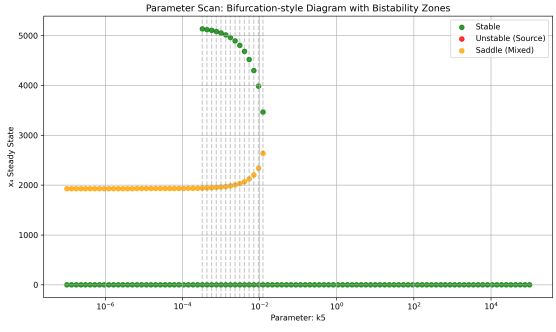

Nullcline: $k_5 = 0$ Sweep: k_5

Figure 14: Parameter k_5: elimination vs sweep

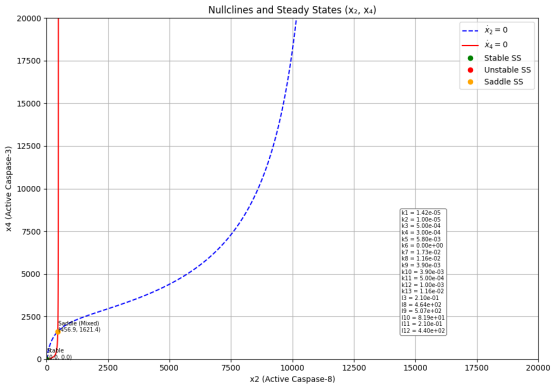

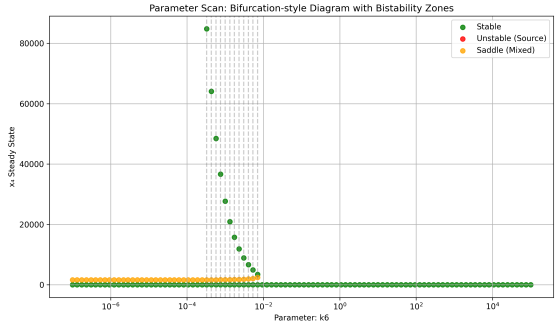

Nullcline: $k_6 = 0$ Sweep: k_6

Figure 15: Parameter k_6: elimination vs sweep

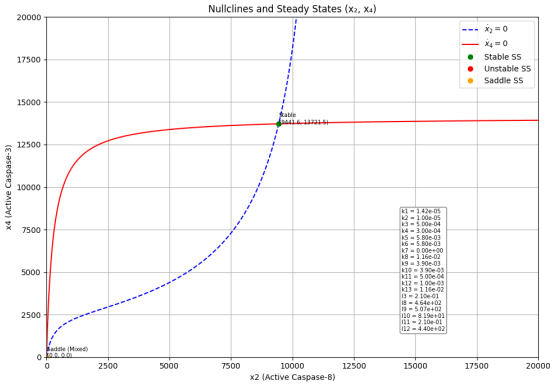

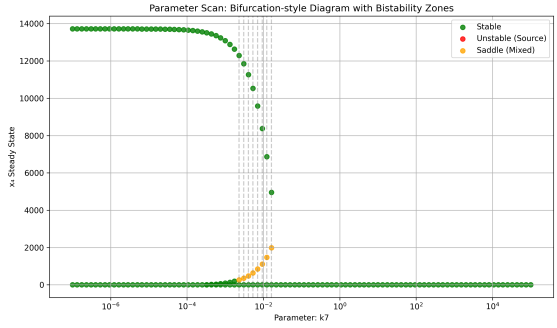

Nullcline: $k_7 = 0$ Sweep: k_7

Figure 16: Parameter k_7: elimination vs sweep

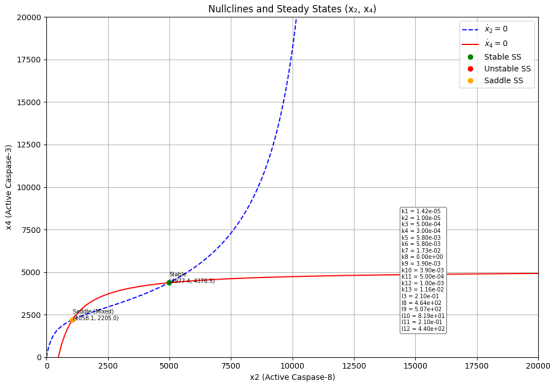

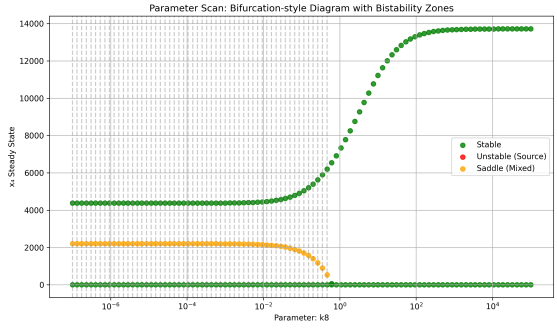

Nullcline: $k_8 = 0$ Sweep: k_8

Figure 17: Parameter k_8: elimination vs sweep

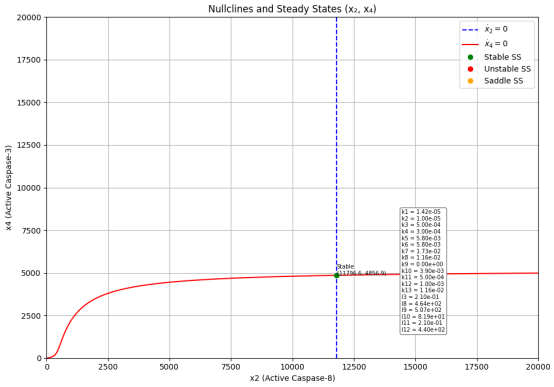

Nullcline: $k_9 = 0$

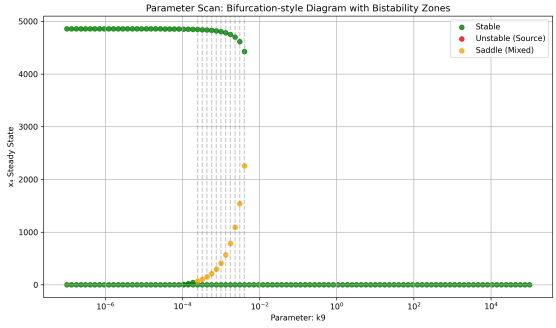

Sweep: k_9

Figure 18: Parameter k_9: elimination vs sweep

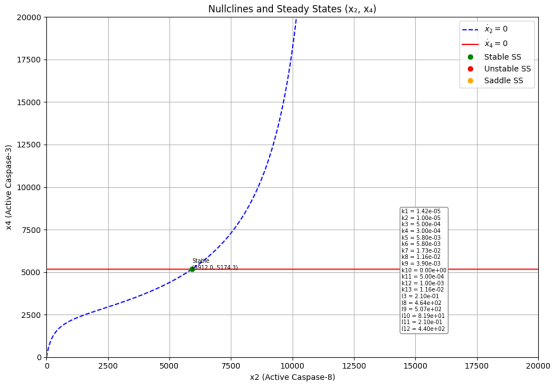

Nullcline: $k_{10} = 0$

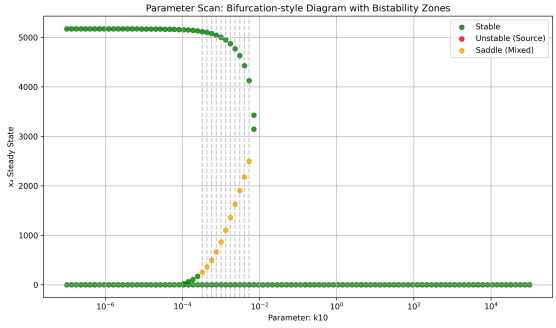

Sweep: k_{10}

Figure 19: Parameter k_{10}: elimination vs sweep

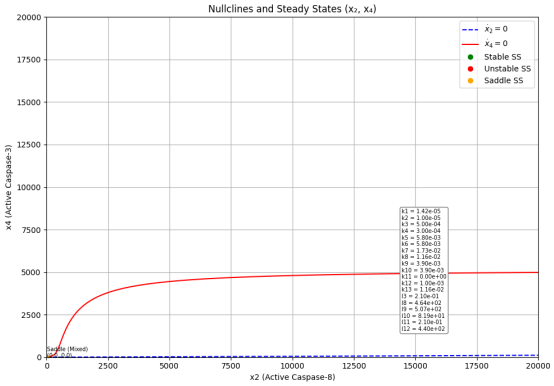

Nullcline: $k_{11} = 0$

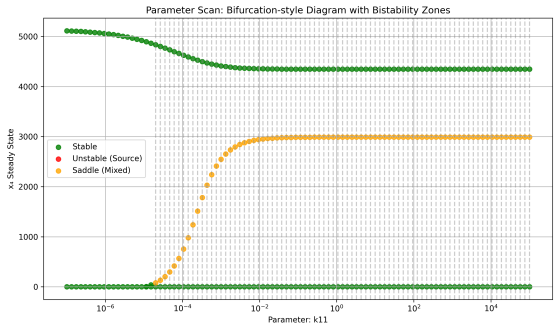

Sweep: k_{11}

Figure 20: Parameter k_{11}: elimination vs sweep

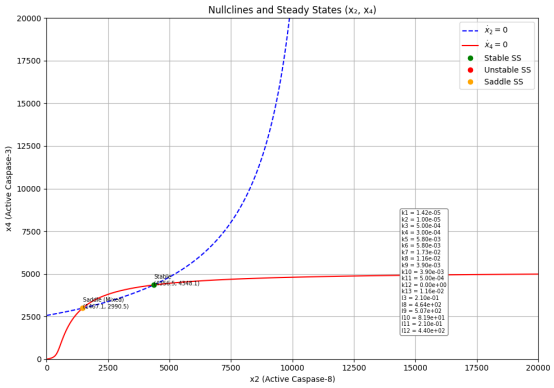

Nullcline: $k_{12} = 0$

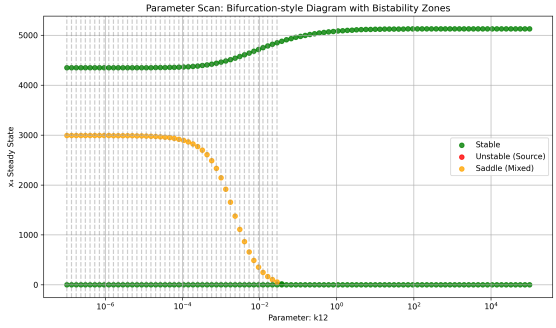

Sweep: k_{12}

Figure 21: Parameter k_{12}: elimination vs sweep

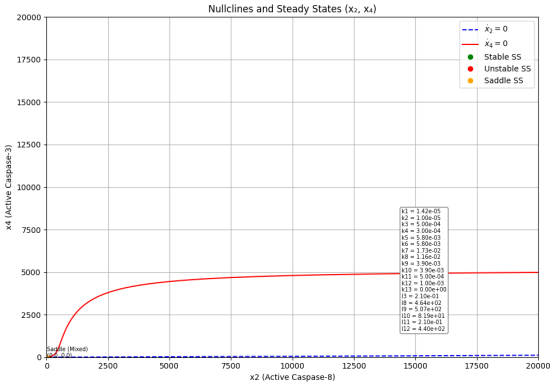

Nullcline: $k_{13} = 0$

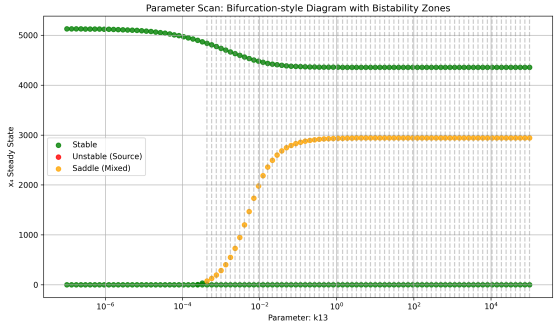

Sweep: k_{13}

Figure 22: Parameter k_{13}: elimination vs sweep

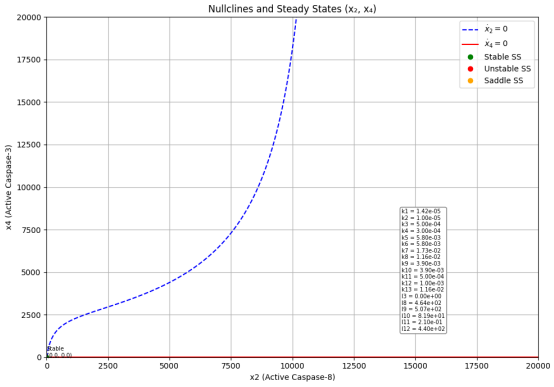

Nullcline: $\ell_3 = 0$

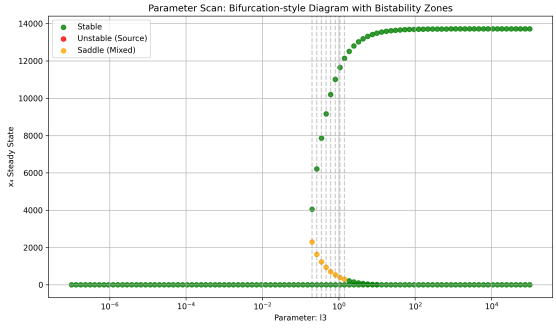

Sweep: ℓ_3

Figure 23: Parameter ℓ_3: elimination vs sweep

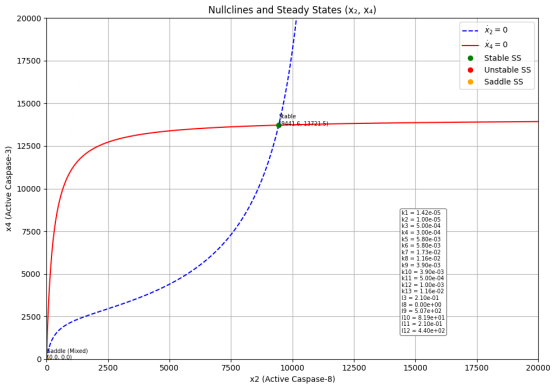

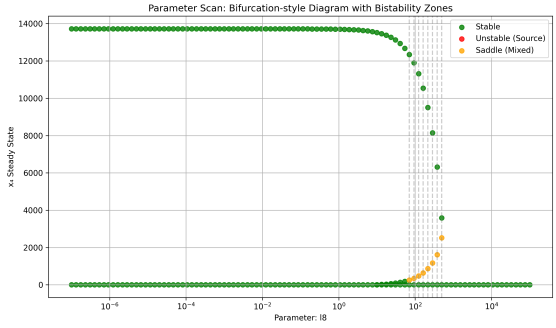

Nullcline: $\ell_8 = 0$ Sweep: ℓ_8

Figure 24: Parameter ℓ_8: elimination vs sweep

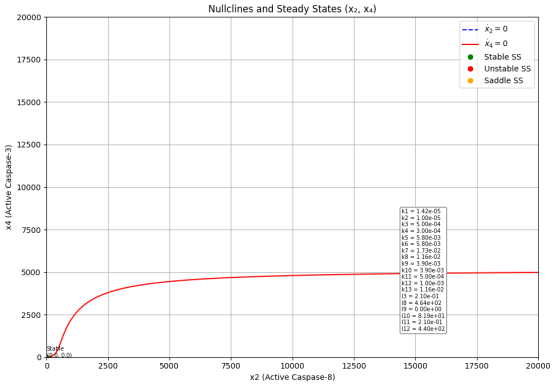

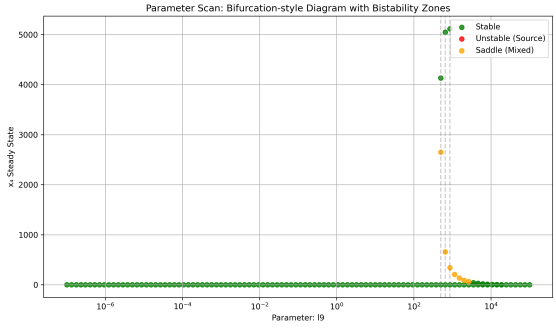

Nullcline: $\ell_9 = 0$ Sweep: ℓ_9

Figure 25: Parameter ℓ_9: elimination vs sweep

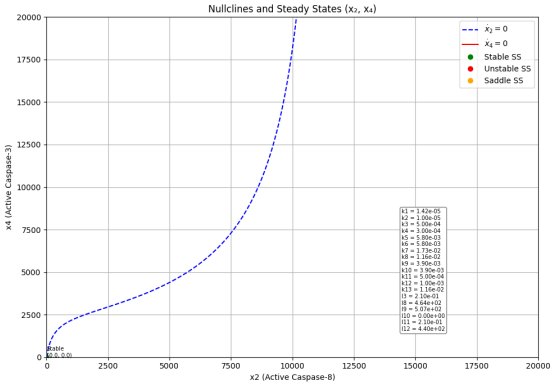

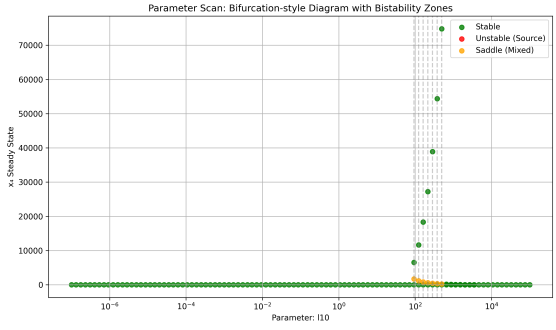

Nullcline: $\ell_{10} = 0$ Sweep: ℓ_{10}

Figure 26: Parameter ℓ_{10}: elimination vs sweep

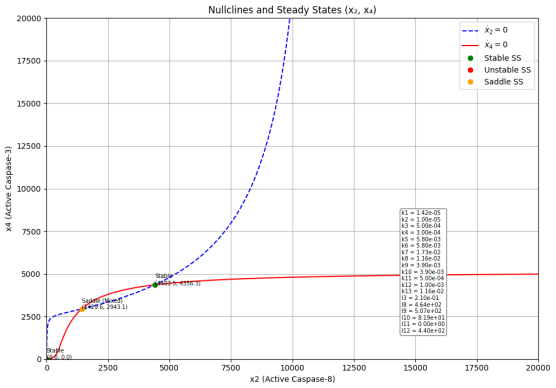

Nullcline: $\ell_{11} = 0$

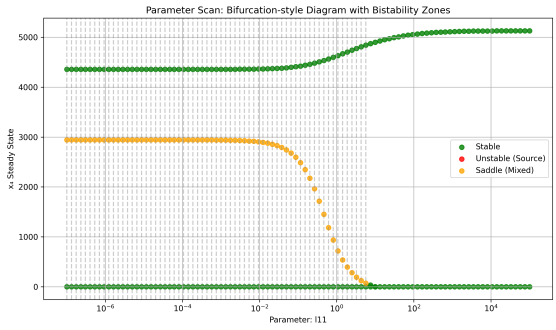

Sweep: ℓ_{11}

Figure 27: Parameter ℓ_{11}: elimination vs sweep

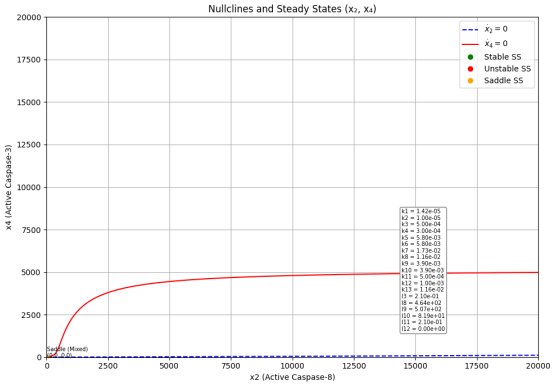

Nullcline: $\ell_{12} = 0$

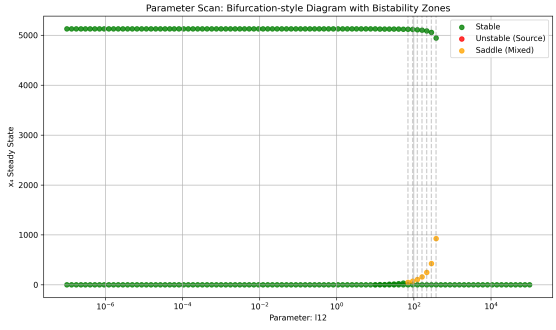

Sweep: ℓ_{12}

Figure 28: Parameter ℓ_{12}: elimination vs sweep

References

[1] Tilo Eissing, Holger Conzelmann, Ernst Dieter Gilles, Frank Allgöwer, Eric Bullinger, and Peter Scheurich. Bistability analyses of caspase activation in a model for fas-induced apoptosis. *Biophysical Journal*, 86(3):1647–1659, 2004.

[2] J.W. Stucki and R. Somogyi. Bistability and irreversible switching in biochemical networks. *FEBS Letters*, 588(15):2456–2462, 2014.

[3] Stefan Waldherr and Frank Allgöwer. Sensitivity analysis and model reduction for a caspase activation model. *BMC Systems Biology*, 1(1):6, 2007.

[4] Megan Dowdell. Python simulations: Symbolic and numerical analysis of apoptotic bistability. `https://github.com/megandowdell/caspasebistability`, 2025. July 2025.

[5] Aaron Meurer, Christopher P. Smith, Mateusz Paprocki, Ondřej Čertík, Sergey B. Kirpichev, Matthew Rocklin, AMiT Kumar, Sergiu Ivanov, Jason K. Moore, Sartaj Singh, et al. Sympy: symbolic computing in python. *PeerJ Computer Science*, 3:e103, 2017.

[6] Charles R. Harris, K. Jarrod Millman, Stéfan J. van der Walt, Ralf Gommers, Pauli Virtanen, David Cournapeau, Eric Wieser, Julian Taylor, Sebastian Berg, Nathaniel J. Smith, et al. Array programming with NumPy. *Nature*, 585(7825):357–362, 2020.

[7] J. D. Hunter. Matplotlib: A 2d graphics environment, 2007.

[8] Steven H. Strogatz. *Nonlinear Dynamics and Chaos: With Applications to Physics, Biology, Chemistry, and Engineering*. Westview Press, 2 edition, 2015.

[9] John G. Albeck, Jason M. Burke, Bree B. Aldridge, Ming Zhang, Douglas A. Lauffenburger, and Peter K. Sorger. Quantitative analysis of pathways controlling extrinsic apoptosis in single cells. *Molecular Cell*, 30(1):11–25, 2008.

[10] James E Ferrell. Self-perpetuating states in signal transduction: positive feedback, double-negative feedback and bistability. *Current Opinion in Cell Biology*, 14(2):140–148, 2002.

Acknowledgments:

REU Faculty Mentor Anne Shiu; TAMU Department of Mathematics; NSF REU program.

REU Graduate Student Mentor Zeytoon Kazemimoghaddam; TAMU Department of Mathematics; NSF REU program.